

# Electronic resonances in expanding non-neutral ultracold plasma

S. Ya. Bronin,<sup>1</sup> E. V. Vikhrov,<sup>1</sup> S. A. Saakyan,<sup>1,2</sup> B. B. Zelener,<sup>1</sup> and B. V. Zelener<sup>1,\*</sup>

<sup>1</sup>*Joint Institute for High Temperatures of the Russian Academy of Sciences,  
Izhorskaya St. 13, Bldg. 2, Moscow 125412, Russia*

<sup>2</sup>*National Research University Higher School of Economics (NRU HSE), Myasnitskaya St. 20, Moscow 101000, Russia*

(Dated: December 25, 2023)

Calculations of the spectrum of eigen oscillations of an inhomogeneous ultracold plasma are presented both in the absence and in the presence of charge imbalance. The collective modes of these plasma oscillations are recorded in experiments as absorption resonances of a radio frequency electric field. It is shown that in the presence of friction of the electronic component, a discrete spectrum of plasma eigen oscillations is formed. The dependence of the frequency of these resonances on the plasma expansion time in the presence of a charge imbalance was obtained. There is good agreement with the experiments of different authors.

## I. INTRODUCTION

Experimental study of ultracold plasma (UCP) makes it possible to find the basic physical mechanisms of the processes occurring in any fully ionized plasma, both in case of stationary conditions and during plasma expansion. This is due to the well-controlled initial conditions and relatively slow expansion dynamics. In addition, only the Coulomb interaction between particles is essential in the UCP, while other interactions can be neglected. At present, a fairly large amount of experimental data have been obtained for the UCP of various chemical elements (Xe, Sr, Rb, Ca) with various densities, various numbers of particles, and various initial temperatures of electrons and ions. Many theoretical papers devoted to this field have also been published (see reviews [1, 2]). Most of the experimental results for the UCP are associated with the study of ions, for which various diagnostic methods, including optical methods, have been developed. For the study of electrons, diagnostic methods are associated with the use of constant and alternating electric fields. In [3, 4], the process of electron evaporation was studied by means of constant electric field in the xenon UCP, that is, the escape of a part of the electrons from the plasma cloud.

Results were obtained for the fraction of remaining electrons as a function of the number of particles, density and the initial kinetic energy of the electrons. In [5], in addition to a constant field, a radio-frequency field with frequency of 5 to 40 MHz and with wavelength much larger than the plasma size was also used to study electrons in the UCP of xenon atoms. By means of scanning the frequency of the rf field within the said range at various times of the plasma expansion, the authors of [5] recorded the resonant signal of the electron output at a certain frequency. Authors of [6] observed in the xenon UCP collective modes which were excited by radio-frequency electric fields and were detected by means of enhanced electron emission during plasma expansion. In

[2, 5–8], dependences of the resonant frequencies of electrons on the charge imbalance in the UCP were obtained. Analysis of the results of experiments by means of an rf electric field requires a study of eigen oscillations of an inhomogeneous non-neutral plasma. The first studies of this kind [9–11] are devoted to bounded plasmas with cylindrical symmetry, where the electron component is confined by a strong magnetic field. A detailed description of these studies is given in the monograph [12]. Papers [13, 14] are devoted to the study of eigen oscillations of a spherically symmetric bounded plasma, in which the electronic component is held by an electric field caused by a charge imbalance. As shown in [14], in the absence of friction, i.e. momentum transfer from the electronic component to the ion one, the spectrum of eigen vibrations is continuous. In [13] the levels of the fundamental mode of plasma eigen oscillations at the beginning of expansion ( $t = 0$ ) were obtained depending on the charge imbalance. The interaction of plasma with a radio frequency field was simulated using molecular dynamics method. However, it was not possible to describe the dependence of the spectrum on the imbalance and plasma density during plasma expansion, as was observed in experiments [5, 6].

In this paper we use a method based on solving the known equation for the electric field. This takes into account the interaction of the field with the plasma by means of conductivity  $\mu(\omega, \mathbf{r})$  and dielectric permittivity  $\varepsilon(\omega, \mathbf{r})$  ( $\omega$  is frequency of the rf electric field), which relate the local values of the current density and electric induction to the local value of the electric field intensity. Such statement of the problem limits the range of its applicability to conditions assuming that the mean free path of electron is small compared to the characteristic length of the field variation. The calculations were performed in relation to the experimental conditions [5, 6]. The use of this method allowed us to explain the dependence of the spectrum of eigen oscillations of a spherical plasma on the charge imbalance and on the expansion time. At the same time, good agreement with experimental data was obtained [5, 6].

---

\* bzelener@mail.ru

## II. CALCULATION MODEL

The calculations are performed for the experimental conditions of [5, 6]. We consider the plasma that emerges upon single ionization of a limited volume of a cooled neutral gas ( $\sim 1$  mK). Characteristic initial dimensions of the plasma  $\sigma_0$  in experiments are limited to fractions of a centimeter, the number of ions and electrons  $N_i$ ,  $N_e$  are from  $10^4$  to  $10^8$  and the temperature  $T_e$  of electrons formed during the ionization is between one and few hundred degrees Kelvin. At the initial stages of the free expansion of the plasma over times of the order of  $\sigma_0/v_{T_e}$  ( $v_{T_e}$  is the thermal speed of electrons), that is, of the order of fractions of a microsecond, fast electrons leave the plasma. The resulting charge imbalance creates an electric field that prevents further leakage of electrons, therefore  $\Delta N = N_i - N_e$  remains constant. In order to calculate  $\Delta N$ , the results of [3, 15] are used. Plasma expansion takes place at a rate characteristic for the ion component, which are several orders of magnitude lower than that for the electron component. This makes it possible to consider the configuration of the ion component as quasi-stationary when studying [15] the motion of the electronic component of the plasma. In particular, in consideration of the motion of the electronic component, the current value of the plasma size  $\sigma(t)$  ( $\sigma(0) = \sigma_0$ ) is assumed to be constant. This said size is determined by the equality  $\sigma_0(t) = \sqrt{\langle r^2 \rangle / 3}$  where angular brackets denote averaging over the ionic configuration. We consider interaction of the electronic component with an electromagnetic field whose wavelength is much larger than the plasma size, which makes it possible to neglect the influence of the vector potential.

In the linear approximation for potential  $\Phi$ , the electric field  $\mathbf{E} = -\nabla\Phi \exp(i\omega t)$  arising under the action of an external field  $\mathbf{E}_0 = \mathbf{k}E_0 \cos(\omega t)$  (the field corresponds to the orbital number  $l = 1$ ;  $\mathbf{k}$  is the unit vector along the  $z$  axis) is determined by the following equation:

$$\nabla(\varepsilon \nabla \Phi) = 0. \quad (1)$$

Here the permittivity is related to the conductivity  $\mu$  as follows [16]:

$$\begin{aligned} \varepsilon &= 1 - \frac{4\pi i}{\omega} \mu = \varepsilon_1 + i\varepsilon_2 \\ \mu &= \mu_1 + i\mu_2 \sim n_e(r), \end{aligned} \quad (2)$$

where  $n_e(r)$  is the electron density.

Setting  $\Phi = (\varphi_1 + i\varphi_2) \exp(i\omega t)$  into equation (1), we obtain a system of second-order linear equations (A7) for the functions  $\varphi_1$  and  $\varphi_2$ , with two boundary conditions in the center and two at infinity (the complete derivation of the system of equations (A7) is presented in Appendix A):

$\varphi_1(0) = \varphi_2(0) = 0$  at  $r = 0$ ,  $\varphi_1 + E_0 r \rightarrow 0$ ,  $\varphi_2 \rightarrow 0$  at  $r \rightarrow \infty$ .

In our calculations, the region where the electron concentration differs from zero is limited. At  $r < x_0\sigma$ ,

$n_e \sim \exp(-r^2/2\sigma^2)$ ; at  $x_0\sigma < r < R = (x_0 + 1/x_0)\sigma$ , concentration varies linearly from  $n_e(x_0\sigma)$  to zero while remaining smooth at the point  $x_0\sigma$ . The fact that the concentration in the region  $r > R$  is zero makes it possible to replace the boundary conditions at  $r \rightarrow \infty$  by equivalent conditions at  $r = R$ :

$$\begin{aligned} 2\varphi_1 + R\varphi_1' &= -3E_0 \\ 2\varphi_2 + R\varphi_2' &= 0. \end{aligned} \quad (3)$$

The chosen scheme for numerical calculation of equations (A7) consists in selecting  $\varphi_1'(0)$  and  $\varphi_2'(0)$  which would fulfill the boundary conditions at  $r = R$ . With this calculation scheme, the admissible values of  $x_0$  are determined by the accuracy of the computing device employed, since the accuracy of determining  $\varphi_1'(0)$  and  $\varphi_2'(0)$  is limited by the number of binary digits in the representation of numbers. In our case, the allowed values of  $x_0$  should not exceed  $x_0 = 3$ .

Numerical solution of equations (A7) (Appendix A) makes it possible to determine the conditions for an increase of heat release in the plasma, which is accompanied in the experiment by an increase in the registered flux of electrons leaving the plasma region. The total heat release is given by the integral (B5) (see Appendix B). As the frequency of the external electric field approaches the frequency of eigen oscillations, the heat release tends to infinity, which makes it possible to determine the spectrum of eigen oscillations of the plasma under study.

## III. ABSORPTION RESONANCES AT $\Delta N = 0$

First, let's consider the case of a small imbalance ( $\Delta N = 0$ ), when the electric field generated by it can be neglected. In this case, the frequency dependence of conductivity and permittivity is given by the known relations [16]:

$$\begin{aligned} \mu &= \frac{e^2 n_e(r)}{m_e} \frac{\omega}{\omega\nu + i\omega^2} \\ \varepsilon &= 1 - \frac{\omega_p^2(r)}{\omega^2 - i\omega\nu}, \end{aligned} \quad (4)$$

where  $\nu$  is frequency of electron-ion collisions and  $\omega_p(r) = \sqrt{4\pi e^2 n_e(r)/m_e}$ . The value of  $\nu$  is calculated by means of the formula for a weakly coupled plasma [17]:

$$\begin{aligned} \nu &= \frac{4\sqrt{2}\pi n_i e^2 \ln\Lambda}{3\sqrt{m_e T_e^3}} \\ \ln\Lambda &= \ln \frac{1}{\sqrt{3}\Gamma_e^3} \\ \Gamma_e &= \frac{e^2 \sqrt[3]{4\pi n_e/3}}{T_e}, \end{aligned} \quad (5)$$

where  $T_e$  is equal to the average electron temperature in the plasma region and  $n_i$  is ionic concentration. The

condition for the applicability of (4) is the smallness of the free path of electrons in comparison with the characteristic length of the electric field inhomogeneity  $d$ :

$$d \gg v_{T_e}/\nu, \quad (6)$$

where  $v_{T_e}$  is thermal electron velocity.

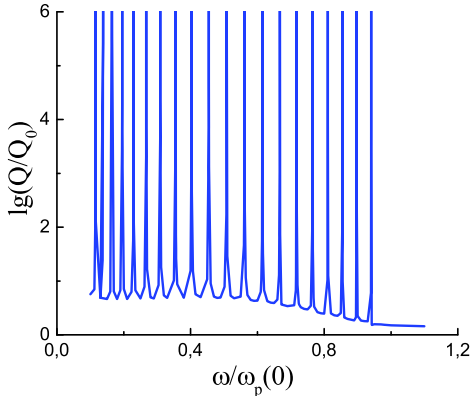


FIG. 1. Dependence logarithm of dimensionless  $Q/Q_0$  on  $\omega/\omega_p(0)$  at  $\nu = 0.4\omega_p(0)$ ,  $x_0 = 3$ .

The solution of equations (A7) with boundary conditions (3) describe the plasma response to the effect of external rf radiation with a frequency of  $\omega$  and an amplitude of  $E_0$ . Figure 1 shows the dependence of heat release  $Q/Q_0$  where  $Q_0 = E(0)^2 \int \mu_1 d\mathbf{r}/2$  on  $\omega/\omega_p(0)$  at  $\nu = 0.4\omega_p(0)$ . Calculations demonstrate distinct heat release resonances, similar to Tonks-Dattner resonances. The same resonances of heat release were observed in calculations [13] performed by the method of molecular dynamics. When the resonant frequency  $\tilde{\omega}$  is approached, the heat release grows inversely proportional to the square of the distance from the resonance  $Q \sim 1/(\omega - \tilde{\omega})^2$ .

The solutions of equations (A7)  $\varphi_1$  and  $\varphi_2$  also increase indefinitely inversely  $\omega - \tilde{\omega}$ , and the limits of the products  $(\omega - \tilde{\omega})\varphi_{1,2}$  for  $\omega \rightarrow \tilde{\omega}$  equal to  $\tilde{\varphi}_{1,2}$  are solutions of homogeneous equations (A7) (with  $E_0 = 0$ ), that is, they represent the eigen oscillations of the plasma formation under consideration. In fact, the lifetime of real oscillations with a resonant frequency is limited by the condition of quasi-stationarity and does not exceed the interval  $\Delta t$ , within which the ion distribution can be considered unchanged. Accordingly, the width of the observed resonance cannot be less than  $\Delta\omega = 2\pi/\Delta t$ . The frequencies of such states form a discrete spectrum containing an apparently infinite number of frequencies in the region  $\omega < \omega_p(0)$ .

Figure 2 shows an example of a solutions of homogeneous equations (A7) normalized by means of the equality  $\int (\tilde{\varphi}_1^2 + \tilde{\varphi}_2^2) r^2 dr / \sigma^3 = 1$  corresponding to the tenth resonance ( $\tilde{\omega} = 0.51 \dots \omega_p(0)$ ). The blue curve corresponds to the function  $\tilde{\varphi}_1$ , the red curve corresponds to the function  $\tilde{\varphi}_2$ . The number of extrema of the function  $\tilde{\varphi}_2$  is

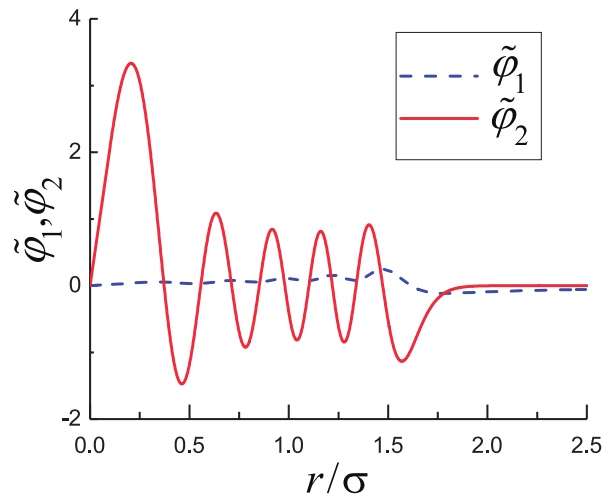


FIG. 2. Normalized eigensolutions of homogeneous equations (11) corresponding to the eigen frequency  $\omega/\omega_p(0) = 0.51$  for  $\omega_0 = 0$ ,  $\nu = 0.4\omega_p(0)$ ,  $x_0 = 3$  depending on  $r/\sigma$ :  $\tilde{\varphi}_1$  is the blue curve,  $\tilde{\varphi}_2$  is the red curve.

equal to the serial number  $N$  of resonances, numbered from right to left. Choosing  $\sigma/N$  as the characteristic size of the field inhomogeneity, we obtain from the inequality (5), which determines the range of applicability of the equations considered, the following estimate for the maximum number of eigen frequencies:

$$N < \sigma\nu/v_{T_e}. \quad (7)$$

With  $\nu/\omega_p(0)$  decreasing, the distance between eigen frequencies decreases. Figure 3 shows eigen frequencies  $\omega_n(\nu)$ , numbered starting from the maximum frequency  $\omega_1 \approx \omega_p$ , for two values of the friction coefficient:  $\nu/\omega_p(0) = 0.4$  is for the blue dash curve and  $\nu/\omega_p(0) = 0.1$  is for the red solid curve.

For small friction coefficients, the calculations are impossible due to the same reasons as for large values of  $x_0$ . Calculations for  $\nu/\omega_p(0)$  values greater than 0.1 show that the distance between resonant frequencies decreases with decreasing friction coefficient which agrees with the well-known fact that in the absence of friction the spectrum is continuous [14], similarly to the Trivelpiece-Gould spectrum [10].

#### IV. CALCULATION OF ABSORPTION RESONANCES WITH ACCOUNT TAKEN OF THE CHARGE IMBALANCE

In order to calculate the spectrum of eigen oscillations of an inhomogeneous plasma, with account taken of the charge imbalance, it is necessary to determine the conductivity and dielectric permittivity of the plasma in the presence of a constant electric field. A similar problem was solved in [10] for the conditions where the electronic component is confined by means of a magnetic field. Af-

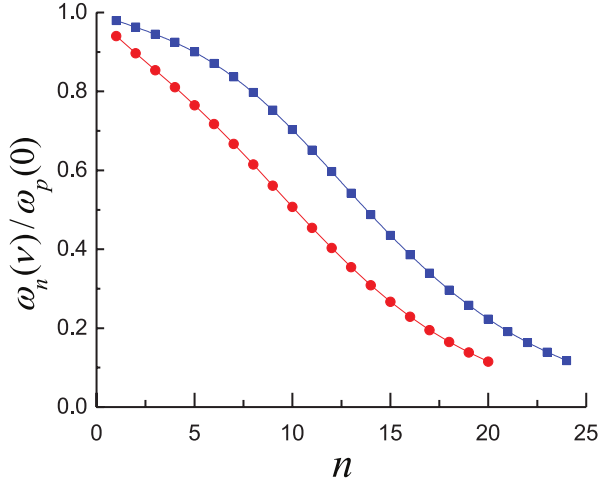


FIG. 3. eigen frequencies  $\omega_n(\nu)/\omega_p(0)$ , where  $n$  is the serial number of the resonance, for  $\omega_0 = 0$  and for two values of the friction coefficient:  $\nu/\omega_p(0) = 0.1$  corresponds to the blue curve and 0.4 corresponds to the red curve.

ter a quasi-stationary mode for the electric field is established in the presence of spherical symmetry, the following self-similar expression is valid [15]:

$$\mathbf{E}_{st}(\mathbf{r}, t) = \frac{e\Delta N}{\sigma^3(t)} \mathbf{r} \eta \left( \frac{r}{\sigma(t)} \right), \quad (8)$$

where  $\eta(\rho)$  is constant in the inner part of the plasma and, decreases proportionally to  $1/\rho^3$  outside it. For the potential energy of electrons, we have:

$$\begin{aligned} e\varphi_{st} &= \frac{e^2\Delta N}{\sigma^3(t)} \int_0^r r' \eta(r'/\sigma(t)) dr' \\ &\approx \frac{e^2\Delta N}{\sigma^3(t)} \eta(0) \frac{r^2}{2} = \frac{m_e \omega_0^2(t)}{2} r^2. \end{aligned} \quad (9)$$

With account taken of the following estimates:  $\eta(0) \approx 1$ ;  $\Delta N \approx \sqrt{kT_e N_i \sigma_0}/e$  [3, 15], we obtain:

$$\omega_0^2(t) \approx \frac{e\sqrt{kT_e N_i \sigma_0}}{m_e \sigma^3(t)}. \quad (10)$$

Let us represent the solution of the equation of motion of an individual electron in an external electric field  $\mathbf{E} = \mathbf{E}(\mathbf{r}) \exp(i\omega t)$ , with account taken of the friction coefficient  $\nu$ :

$$m_e \ddot{\mathbf{r}} + m_e \mathbf{r} \omega_0^2 + m_e \nu \dot{\mathbf{r}} = -e \mathbf{E}(\mathbf{r}) e^{i\omega t} \quad (11)$$

in following form:

$$\mathbf{r}(t) = \mathbf{r}_0(t) + \Delta \mathbf{r}(t) \quad (12)$$

where  $\mathbf{r}_0(t)$  is the solution of this equation for  $\mathbf{E}(\mathbf{r}) = 0$  and

$$\Delta \mathbf{r}(t) = -\frac{e}{m_e \omega_1} \int_0^t e^{-\nu(t-t')/2} \sin(\omega_1(t-t')) \mathbf{E}(\mathbf{r}(t')) e^{i\omega t'} dt' \quad (13)$$

where  $\omega_1^2 = \omega_0^2 - \nu^2/4$ .

In the conditions where the mean free path of electron ( $\nu T_e$  is the thermal velocity of electrons) is less than the characteristic size of the field variation  $d$  (inequality (6)), the following expression is valid for  $\Delta \dot{\mathbf{r}}(t)$ :

$$\begin{aligned} \Delta \dot{\mathbf{r}}(t) &\approx \frac{e}{m_e \omega_1} \mathbf{E}(\mathbf{r}(t)) e^{i\omega t} \\ &\cdot \int_0^\infty e^{-(\nu/2+i\omega t)t} \cdot (\omega_1 \cos \omega_1 t - 0.5\nu \sin \omega_1 t) dt \\ &= -\frac{e\omega}{m_e} \mathbf{E}(\mathbf{r}(t)) e^{i\omega t} \frac{\omega}{\omega\nu - i(\omega_0^2 - \omega^2)}. \end{aligned} \quad (14)$$

For the electron current we have:

$$\mathbf{j}(\mathbf{r}) = \int f(\mathbf{r}(0), \dot{\mathbf{r}}(0)) \dot{\mathbf{r}}(t) d\mathbf{r}(0) d\dot{\mathbf{r}}(0), \quad (15)$$

where  $f(\mathbf{r}(0), \dot{\mathbf{r}}(0))$  is the quasi-equilibrium electron distribution function  $\int f(\mathbf{r}, \dot{\mathbf{r}}) d\dot{\mathbf{r}} = n_e(\mathbf{r})$ , for which the following equality is valid within the linear approximation:  $f(\mathbf{r}(0), \dot{\mathbf{r}}(0)) = f(\mathbf{r}(t), \dot{\mathbf{r}}(t))$ .

After the following change of variables in (15):  $\mathbf{r}(0), \dot{\mathbf{r}}(0) \rightarrow \mathbf{r}(t), \dot{\mathbf{r}}(t)$ , we obtain for the current:

$$\begin{aligned} \mathbf{j}(\mathbf{r}) &= \mu(\mathbf{r}, \omega) \mathbf{E}(\mathbf{r}) e^{i\omega t} \\ \mu(\mathbf{r}, \omega) &= \frac{e^2 n_e(\mathbf{r})}{m_e} \frac{\omega}{\omega\nu - i(\omega_0^2 - \omega^2)} = \mu_1 + i\mu_2, \end{aligned} \quad (16)$$

where  $\mu$  is local plasma conductivity. For the dielectric permittivity we have:

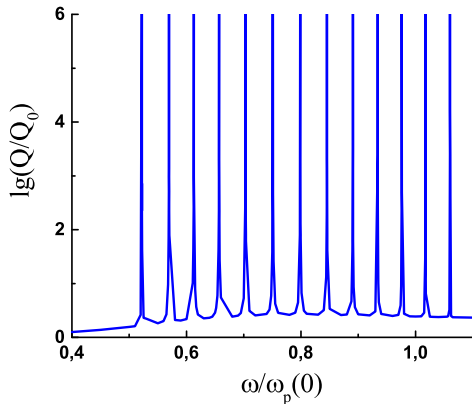
$$\begin{aligned} \varepsilon &= 1 - \frac{4\pi i}{\omega} (\mu_1 + i\mu_2) \\ &= 1 - \frac{\omega_p^2}{\omega^2 - \omega_0^2 - i\omega\nu} = \varepsilon_1 + i\varepsilon_2, \end{aligned} \quad (17)$$

where  $\omega_p = \sqrt{4\pi e^2 n_e(\mathbf{r})/m_e}$  is the plasma frequency.

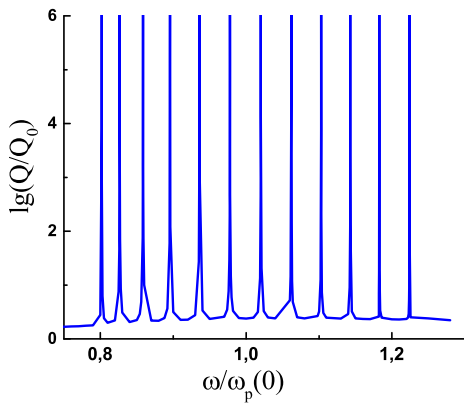
Numerical solution of equations (A7) with dielectric permittivity (17) show that in the presence of friction, the spectrum remains discrete, but with a finite number of eigen frequencies, limited by the minimal frequency  $\sim \omega_0$ . Figure 4 shows the dependence of heat release  $Q$  on  $\omega/\omega_p(0)$  at  $\nu = 0.4\omega_p(0)$  and  $\omega_0 = 0.5\omega_p(0)$  (4(a)) and  $\omega_0 = 0.8\omega_p(0)$  (4(b)) with all eigen frequencies. The minimum of the resonant frequency is close to  $\omega = \omega_0$ . It follows from the above-said expression for the frequency  $\omega_0$  that its time dependence is determined by the following relation:  $\omega_0 \sim \sqrt{\Delta N/\sigma(t)^3}$ . A similar time dependence of the resonant frequency was observed in experiments [7]. In the stationary expansion mode, where  $\Delta N$  and the plasma expansion velocity reach stationary values ( $\sigma(t) \sim t$ ), the following relation is valid for time dependence of the frequency  $\omega_0$ :  $\omega_0 \sim t^{-3/2}$ .

## V. COMPARISON WITH EXPERIMENT

Figure 5 shows the results of our calculation of the frequencies of the main resonances  $\omega_0$  on the basis of



(a)



(b)

FIG. 4. Dependence of the logarithm of the dimensionless quantity  $Q/Q_0$  on  $\omega/\omega_p(0)$  at  $\nu = 0.4\omega_p(0)$   $x_0 = 3$ : (a)  $\omega_0 = 0.5\omega_p(0)$ ; (b)  $\omega_0 = 0.8\omega_p(0)$ ;

(9) in comparison with the experiment [5]. The ratio  $\omega_0(t)/\omega_p(0, t)$  does not depend on time. The experimental values are obtained by means of digitizing Fig. 1 of [5]. Unfortunately, for other parameters of the xenon UCP, [5] does not provide resonance frequencies, but only gives the results of processing for the expansion time dependence of the average density.

Figure 6 shows the results of our calculations of the fundamental frequencies of electronic resonances  $\omega_0$  and the frequencies of the first three modes on the basis of (A7) with dielectric permittivity (17), in comparison with experiment [6]. The ratio  $\omega_0(t)/\omega_p(0, t)$  in these conditions is 0.25 ( $\sigma_0 = 0.028$  cm,  $n_0 = 2 \cdot 10^9$  cm $^{-3}$ ,  $T_e = 100$  K). The lower curve (the main resonance  $\omega_0$ ) is calculated by means of (17). The other three curves are obtained from the above-described calculations for the ratios of the next resonances to the main resonance  $\omega_k/\omega_0$ . The curve following the first one corresponds to the 1st experimental resonance from [6], the next curve corresponds to the 2nd experimental resonance from [6],

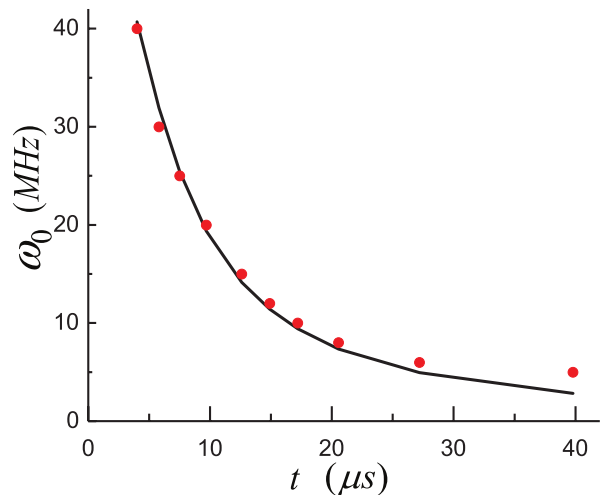


FIG. 5. Comparison of calculations with experiment [5]. Points are for the experiment, the curve is for the calculation (9). UCP parameters:  $\sigma_0 = 0,022$  cm,  $N_i = 8 \cdot 10^4$ ,  $T_{e0} = 26$  K

and the last curve corresponds to the 3rd experimental resonance from [6]. Agreement with experiments [5, 6] can be considered good.

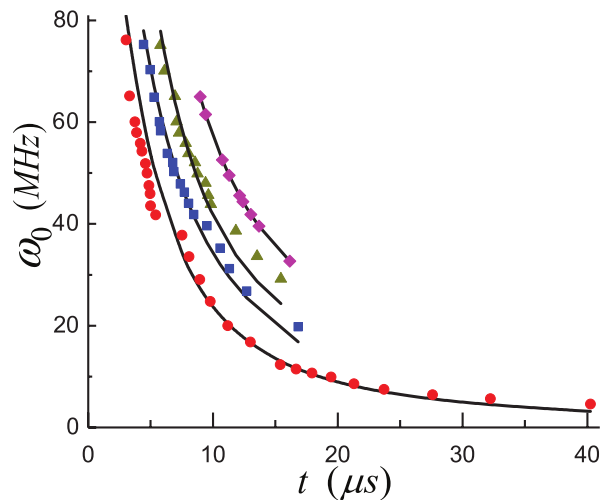


FIG. 6. Comparison of calculations with experiment [6]. Points are for the experiment, the lower curve is for calculation (17); the next curves are from numerical solution of (??) with dielectric permittivity (17). UCP parameters:  $\sigma_0 = 0.028$  cm,  $N_i = 1.5 \cdot 10^6$ ,  $T_e = 100$  K,  $\nu_{ei0} = 24$  MHz.

## VI. CONCLUSION

In the present paper, the spectrum of eigen oscillations of a spherical plasma is obtained as a function of charge imbalance. A method is used which is based on solving the well-known equations for electric field whose interaction with plasma is taken into account by means

of dielectric permittivity  $\epsilon(\omega, \mathbf{r})$  (where  $\omega$  is frequency of the ref field). The range of applicability of this approach is limited by the conditions that assume that the mean free path of electrons is small compared to the characteristic length of the field variation. As a result, the main and subsequent modes of resonances in expanding non-neutral ultracold plasma were obtained, which are in good agreement with the available experimental data. Moreover, such calculations are absent in works devoted to this topic. In addition, we were able to show that electronic resonances also arise in the case of a neutral, but not homogeneous, plasma.

## VII. ACKNOWLEDGMENTS

The research was supported by the Russian Science Foundation Grant No. 21-72-00011 in the part of processing and analysis of the experiment and No. 23-72-10031 in the part of large-scale reworked this article within the framework of the new grant. This work was supported by the Ministry of Science and Higher Education of the Russian Federation (State Assignment No. 075-01129-23-00) in the part of creating a program code for the numerical solution of a system of two second-order differential equations with complex boundary conditions. This research was also supported by computational resources of HPC facilities at HSE University.

### Appendix A

Here is a description, omitted in the text, of the transition from equation (1) to a system of two real equations (A7) for  $\varphi_1$  and  $\varphi_2$

$$\text{Re} [\nabla(\epsilon \nabla \Phi) e^{i\omega t}] = D_1 \cos(\omega t) + D_2 \sin(\omega t) = 0 \quad (\text{A1})$$

Equations for  $D_1$  and  $D_2$  is obtained by applying the operator  $\nabla$  to the expression in parentheses (A1) and keeping only the real part:

$$\begin{aligned} D_1 &= \epsilon_1 \Delta \Phi_1 - \epsilon_2 \Delta \Phi_2 + \nabla \epsilon_1 \nabla \Phi_1 - \nabla \epsilon_2 \nabla \Phi_2 = 0 \\ D_2 &= -\epsilon_1 \Delta \Phi_2 - \epsilon_2 \Delta \Phi_1 - \nabla \epsilon_1 \nabla \Phi_2 - \nabla \epsilon_2 \nabla \Phi_1 = 0 \end{aligned} \quad (\text{A2})$$

A system of second-order linear differential equations with coefficients  $\alpha$  and  $\beta$  for  $\Phi_1$  and  $\Phi_2$  is obtained by combining  $D_1$  and  $D_2$  with  $\epsilon_1$  and  $\epsilon_2$ :

$$\begin{aligned} \frac{1}{\epsilon_1^2 + \epsilon_2^2} (\epsilon_1 D_1 - \epsilon_2 D_2) &= \Delta \Phi_1 + \frac{\epsilon_1 \nabla \epsilon_1 + \epsilon_2 \nabla \epsilon_2}{\epsilon_1^2 + \epsilon_2^2} \nabla \Phi_1 + \frac{\epsilon_2 \nabla \epsilon_1 - \epsilon_1 \nabla \epsilon_2}{\epsilon_1^2 + \epsilon_2^2} \nabla \Phi_2 = 0 \\ -\frac{1}{\epsilon_1^2 + \epsilon_2^2} (\epsilon_2 D_1 + \epsilon_1 D_2) &= \Delta \Phi_2 + \frac{\epsilon_1 \nabla \epsilon_1 + \epsilon_2 \nabla \epsilon_2}{\epsilon_1^2 + \epsilon_2^2} \nabla \Phi_2 - \frac{\epsilon_2 \nabla \epsilon_1 - \epsilon_1 \nabla \epsilon_2}{\epsilon_1^2 + \epsilon_2^2} \nabla \Phi_1 = 0 \end{aligned} \quad (\text{A3})$$

$$\begin{aligned} \frac{\epsilon_1 \nabla \epsilon_1 + \epsilon_2 \nabla \epsilon_2}{\epsilon_1^2 + \epsilon_2^2} &= \alpha \frac{\mathbf{r}}{r} \\ \frac{\epsilon_2 \nabla \epsilon_1 - \epsilon_1 \nabla \epsilon_2}{\epsilon_1^2 + \epsilon_2^2} &= \beta \frac{\mathbf{r}}{r} \end{aligned} \quad (\text{A4})$$

$$\begin{aligned} \alpha &= \frac{\epsilon_1 \epsilon_1' + \epsilon_2 \epsilon_2'}{\epsilon_1^2 + \epsilon_2^2} \\ \beta &= \frac{\epsilon_2 \epsilon_1' - \epsilon_1 \epsilon_2'}{\epsilon_1^2 + \epsilon_2^2} \end{aligned} \quad (\text{A5})$$

In formulas (A6)  $\mathbf{k}$  - the single vector of the z axis :

$$\begin{aligned} \Phi_m &= \varphi_m(r) \cos(\theta) = \varphi_m \frac{\mathbf{r} \mathbf{k}}{r} \\ \nabla \Phi_m &= \frac{\mathbf{r}}{r} \varphi_m' \cos(\theta) + \frac{\mathbf{k}}{r} \varphi_m - \frac{\mathbf{r}}{r^2} \varphi_m \cos(\theta) \\ \frac{\mathbf{r}}{r} \nabla \Phi_m &= \frac{\mathbf{r}}{r} \varphi_m' \cos(\theta) \\ \Delta \Phi_m &= \left( \frac{1}{r^2} \frac{d}{dr} \left( r^2 \frac{d\varphi_m}{dr} \right) - \frac{2}{r^2} \varphi_m \right) \cos(\theta) \end{aligned} \quad (\text{A6})$$

The final expression for the system of second-order linear differential equations for  $\varphi_1$  and  $\varphi_2$  is obtained by using the representation  $\Phi_m$ ,  $\nabla\Phi_m$  and  $\Delta\Phi_m$  through  $\varphi_m$ :

$$\begin{aligned} \frac{1}{r^2} \frac{d}{dr} \left( r^2 \frac{d\varphi_1}{dr} \right) - \frac{2}{r^2} \varphi_1 + \alpha \frac{d\varphi_1}{dr} + \beta \frac{d\varphi_2}{dr} &= 0 \\ \frac{1}{r^2} \frac{d}{dr} \left( r^2 \frac{d\varphi_2}{dr} \right) - \frac{2}{r^2} \varphi_2 + \alpha \frac{d\varphi_2}{dr} - \beta \frac{d\varphi_1}{dr} &= 0 \end{aligned} \quad (\text{A7})$$

### Appendix B

Derivation of the expression for for total heat release (brackets indicate time averaging)  $Q = \int d\mathbf{r} \langle q \rangle$ :

$$q = \text{Re} \mathbf{E} \text{Re} \mathbf{J} = \text{Re} \mathbf{E} \text{Re} (\mu_1 + i\mu_2) \mathbf{E} \quad (\text{B1})$$

The right side of (B1) is transformed using expressions for  $\mathbf{E} = -\nabla\Phi \exp(i\omega t)$  and (16) for  $\mathbf{J}$  :

$$\begin{aligned} &(\mu_1(\nabla\Phi_1 \cos(\omega t) - \nabla\Phi_2 \sin(\omega t)) - \mu_2(\nabla\Phi_1 \sin(\omega t) + \nabla\Phi_2 \cos(\omega t))) \cdot \\ &\quad \cdot (\nabla\Phi_1 \cos(\omega t) - \nabla\Phi_2 \sin(\omega t)) \\ &= \mu_1((\nabla\Phi_1)^2 \cos^2(\omega t) + (\nabla\Phi_2)^2 \sin^2(\omega t)) - \mu_2 \left[ ((\nabla\Phi_1)^2 - (\nabla\Phi_2)^2) \frac{\sin(2\omega t)}{2} \nabla\Phi_1 \Phi_2 \cos(2\omega t) \right] - \\ &\quad - \mu_1 \nabla\Phi_1 \Phi_2 \sin(2\omega t) \end{aligned} \quad (\text{B2})$$

$$\begin{aligned} \langle \cos^2(\omega t) \rangle &= \langle \sin^2(\omega t) \rangle = \frac{1}{2} \\ \langle \cos(2\omega t) \rangle &= \langle \sin(2\omega t) \rangle = 0 \end{aligned} \quad (\text{B3})$$

The expressions for  $\langle q \rangle$  both the function  $\varphi_1$  and  $\varphi_2$  - (B4) and for calculating total heat release  $Q$  - (B5) are obtained by taking into account the equalities (B3) and  $(\nabla\Phi_m)^2$ :

$$\begin{aligned} \langle q \rangle &= \frac{\mu_1}{2} ((\nabla\Phi_1)^2 + (\nabla\Phi_2)^2) \\ (\nabla\Phi_m)^2 &= \frac{\varphi_m^2}{r^2} + \cos^2 \theta \left( \varphi_m'^2 + \frac{\varphi_m^2}{r^2} - \frac{\varphi_m \varphi_m'}{r} \right) + 2\varphi_m \cos^2 \theta \left( \frac{\varphi_m'}{r} - \frac{\varphi_m}{r^2} \right) \\ &= \frac{\varphi_m^2}{r^2} \sin^2 \theta + \varphi_m'^2 \cos^2 \theta \\ \langle q \rangle &= \frac{\mu_1}{2} \left( \sin^2 \theta \frac{\varphi_1^2 + \varphi_2^2}{r^2} + \cos^2 \theta (\varphi_1'^2 + \varphi_2'^2) \right) \end{aligned} \quad (\text{B4})$$

$$Q = \int d\mathbf{r} \langle q \rangle = \frac{2\pi}{3} \int_0^{r_0} \mu_1 \left( \varphi_1^2 + \varphi_2^2 + 2 \cdot r^2 \left\{ \left( \frac{d\varphi_1}{dr} \right)^2 + \left( \frac{d\varphi_2}{dr} \right)^2 \right\} \right) dr. \quad (\text{B5})$$

- 
- [1] Thomas C Killian, T Pattard, T Pohl, and JM Rost. Ultracold neutral plasmas. *Physics Reports*, 449(4-5):77–130, 2007.
  - [2] M Lyon and SL Rolston. Ultracold neutral plasmas. *Reports on Progress in Physics*, 80(1):017001, 2016.
  - [3] TC Killian, S Kulin, SD Bergeson, Luis A Orozco, C Orzel, and SL Rolston. Creation of an ultracold neutral plasma. *Physical Review Letters*, 83(23):4776, 1999.
  - [4] KA Twedt and SL Rolston. Electron evaporation from an ultracold plasma in a uniform electric field. *Physics of Plasmas*, 17(8):082101, 2010.
  - [5] S Kulin, TC Killian, SD Bergeson, and SL Rolston. Plasma oscillations and expansion of an ultracold neutral plasma. *Physical review letters*, 85(2):318, 2000.

- [6] RS Fletcher, XL Zhang, and SL Rolston. Observation of collective modes of ultracold plasmas. *Physical review letters*, 96(10):105003, 2006.
- [7] KA Twedt and SL Rolston. Electronic detection of collective modes of an ultracold plasma. *Physical Review Letters*, 108(6):065003, 2012.
- [8] Truman M Wilson, Wei-Ting Chen, and Jacob L Roberts. Density-dependent response of an ultracold plasma to few-cycle radio-frequency pulses. *Physical Review A*, 87(1):013410, 2013.
- [9] AW Trivelpiece and RW Gould. Space charge waves in cylindrical plasma columns. *Journal of Applied Physics*, 30(11):1784–1793, 1959.
- [10] Adam Dattner. Resonance densities in a cylindrical plasma column. *Physical Review Letters*, 10(6):205, 1963.
- [11] M Gagneaux and PE Vandenplas. Temperature (tonks–dattner) resonances theoretically revisited: New temperature and density diagnostics. *The Physics of fluids*, 29(5):1472–1479, 1986.
- [12] Ronald C Davidson. *Physics of nonneutral plasmas*. World Scientific Publishing Company, 2001.
- [13] Andrei Lyubonko, Thomas Pohl, and Jan-Michael Rost. Collective energy absorption of ultracold plasmas through electronic edge-modes. *New Journal of Physics*, 14:053039, 2012.
- [14] Scott D Bergeson and Ross L Spencer. Neutral-plasma oscillations at zero temperature. *Physical Review E*, 67(2):026414, 2003.
- [15] EV Vikhrov, S Ya Bronin, BB Zelener, and BV Zelener. Ion wave formation during ultracold plasma expansion. *Physical Review E*, 104(1):015212, 2021.
- [16] LD Landau and EM Lifshitz. *Electrodynamics of Continuous Media*. FizMatLit, 1959.
- [17] Lyman Spitzer. *Physics of fully ionized gases*. Courier Corporation, 2006.



